

Distorted magnetic orders and electronic structures of tetragonal FeSe from first-principles

Yong-Feng Li, Li-Fang Zhu, San-Dong Guo, Ye-Chuan Xu, and
Bang-Gui Liu

Institute of Physics, Chinese Academy of Sciences, Beijing 100190, China

Beijing National Laboratory for Condensed Matter Physics, Beijing 100190, China

E-mail: bgliu@mail.iphy.ac.cn

Abstract. We use the state-of-the-arts density-functional-theory method to study various magnetic orders and their effects on the electronic structures of the FeSe. Our calculated results show that, for the spins of the single Fe layer, the striped antiferromagnetic orders with distortion are more favorable in total energy than the checkerboard antiferromagnetic orders with tetragonal symmetry, which is consistent with known experimental data, and the inter-layer magnetic interaction is very weak. We investigate the electronic structures and magnetic property of the distorted phases. We also present our calculated spin coupling constants and discuss the reduction of the Fe magnetic moment by quantum many-body effects. These results are useful to understand the structural, magnetic, and electronic properties of FeSe, and may have some helpful implications to other FeAs-based materials.

PACS numbers: 75.30.-m, 74.10.+v, 75.10.-b, 71.20.-b, 74.20.-z

1. Introduction

The advent of superconducting F-doped LaFeAsO stimulates a world-wide campaign for more and better Fe-based superconductors [1]. More superconductors were obtained by replacing La by other lanthanides or partly substituting F for O, and higher phase-transition temperatures (T_c) were achieved in some of them [2, 3, 4]. Furthermore, more series of Fe-based superconductors were found, including BaFe₂As₂ series and LiFeAs series [5, 6, 7, 8]. The highest T_c in these series reaches 55-56 K in the case of doped SmFeAsO [4]. Various explorations have been performed to elucidate their magnetic orders, electronic structures, superconductivity, and so on [9, 10, 11, 12, 13, 14, 15]. Recently, superconductivity was found even in tetragonal FeSe samples under high pressure and α FeSe phases with Se vacancies [16, 17, 18, 19, 20]. Very recently, SrFeAsF was made superconducting by La and Co doping [21, 22, 23, 24, 25]. The FeSe system is interesting because its FeSe layer is similar to the FeAs layer of the FeAs-based materials: R FeAsO series (R : rare earth elements), A Fe₂As₂ series (A : alkaline-earth elements), LiFeAs series, and SrFeAsF series. In addition to the FeAs layers, there are RO layers in R FeAsO series, A layers in A Fe₂As₂ series, Li layers in LiFeAs series, and SrF layers in SrFeAsF series, but there is nothing else besides the FeSe layers for the FeSe systems. Therefore, it is highly desirable to investigate the magnetic orders, electronic structures, and magnetic properties of the tetragonal FeSe phases (or distorted phases of them).

In this article we use an full-potential density-functional-theory method to study various magnetic orders and their effects on the electronic structures of the FeSe. We suppose checkerboard antiferromagnetic order for the spins of the Fe layer of the tetragonal phase and striped antiferromagnetic orders for those of the symmetry-broken structures, and perform total-energy and force optimization to determine the structural and magnetic parameters. Then, we investigate the corresponding electronic structures and magnetic property of them. Our calculated result means that the striped antiferromagnetic order is favorable for the spins of the Fe layer, which is consistent with main known experimental data. We also discuss the reduction of the Fe magnetic moment by quantum many-body effects. More detailed results are presented in the following.

The paper is organized as follows. In next section, we give our computational detail. In the third section, we present our main DFT calculated results, including optimized magnetic structures and corresponding electronic density of states and energy bands. In the fourth section, we discuss spin interactions and many-body effects on the Fe magnetic moments. Finally, we present our main conclusion in the fifth section.

2. Computational detail

Our calculations are performed by using a full-potential linearized augmented plane wave (FLAPW) method within the density functional theory (DFT)[26], as implemented in

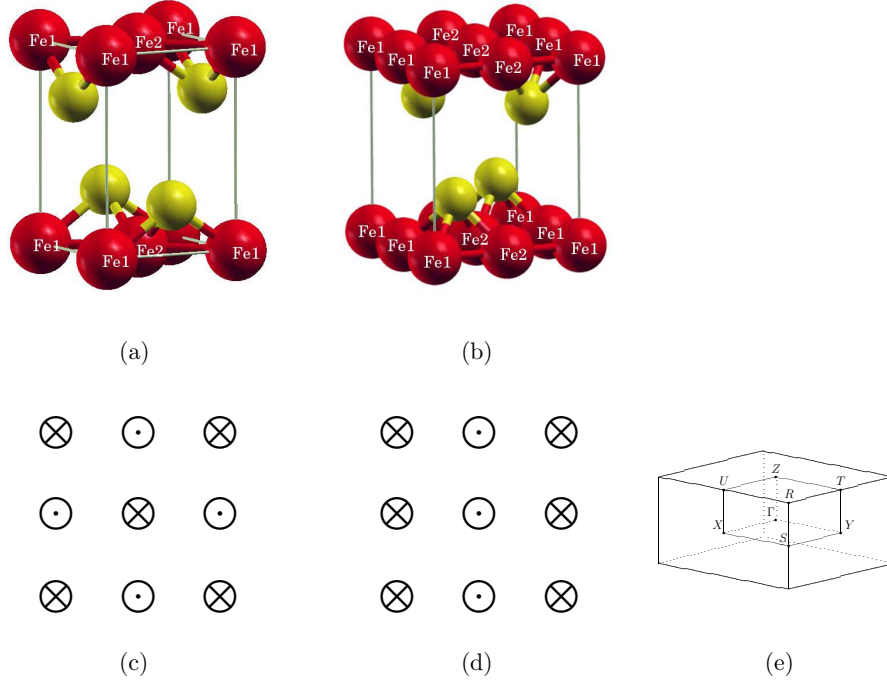


Figure 1. (color online). Schematic structures of tetragonal FeSe (a) and orthorhombic FeSe (b); and the spin configurations of the checkerboard antiferromagnetic order (c) and the striped antiferromagnetic order (d). The big balls with Fe1 and Fe2 indicates the two kinds of Fe atoms with different spin orientations, and the small one Se atom. The sign \otimes means that the Fe1 spin orients upward with respect to the paper plane, and \odot the Fe2 spin downward. The first Brillouin Zone of the orthorhombic FeSe is shown in (e) with the high-symmetry points labelled.

the Vienna package WIEN2k [27]. The generalized gradient approximation (GGA) is used for the exchange and correlation potentials [28]. We take the 3d and 4s states of Fe and the 4s and 4p states of Se as valence states, and the 3p states of Fe and 3d states of Se are treated as semicore states. The core states include all the lower states. The core states are treated in terms of radial Dirac equation and thus the full relativistic effect is included. For the valence and semicore states, the relativistic effect is calculated under the scalar approximation, with spin-orbit interaction being neglected [29]. The radii of Fe and Se muffin-tin spheres are 2.05 and 2.00 a.u., respectively. To get more accurate results, we take $R_{mt} \times K_{max}=9.0$ and make the angular expansion up to $l=10$ in the muffin-tin spheres. We use 1000 k points in the calculations. For different magnetic orders the k points in the first Brillouin zone are chosen differently because of the different symmetry. The self-consistent calculations are controlled by the charge density, and the convergence standard is that the difference between input charge density and output one is less than 0.00005 per unit cell.

We show the unit cell of the tetragonal FeSe (PbO structure) in Fig. 1a. It is a layered structure, in which Fe atom occupies 2a position and Se atom 2c position. There are six possible magnetic configurations for the Fe ions if the tetrahedral FeSe

structure is allowed to distort into orthorhombic structures. Fig. 1e shows the first Brillouin zone with the representative points and lines. The Fe moments in the Fe plane can be arranged to form ferromagnetic or antiferromagnetic orders. The AFM orders can be checkerboard-like (Fig. 1c) or striped (Fig. 1d). For the successive $\{001\}$ planes, the Fe moments can couple ferromagnetically or antiferromagnetically. As a result, we have four different antiferromagnets, namely (a) checkerboard-FM, (b) checkerboard-AF, (c) stripe-FM, and (d) stripe-AF. In addition, when we force Fe moments in the Fe plane have FM order, the self-consistent calculations yield zero moments for the Fe moments, which means that FM order is unstable for FeSe, independent of the interlayer spin arrangements. Therefore, we can actually construct five magnetic orders for this system.

3. Main calculated results

The parameters in our calculations are taken from the experimental values. We use $a = 3.76\text{\AA}$ and $c = 5.52\text{\AA}$. The positions of Se atoms are optimized fully, and the force of Se atom is made less than 2 mRy/a.u. Calculated results of total energy, magnetic moment, and Se position parameter are summarized in Table I. It makes little difference in total energy to arrange interlayer Fe moments in FM or AF order. The total energy results reveal that the intralayer Fe-Fe interaction is strong and the interlayer interaction weak. Actually, the striped arrangement of the Fe moments lowers the total energy of the FeSe layer approximately by 70 meV with respect to the checkerboard arrangement. On the other hand, the non-magnetic order is 154 meV higher than the lowest striped AF order. Therefore, the striped AF spin order is the magnetic ground state in the FeSe layer, but the actual interlayer magnetic interaction is too weak for any density-functional-theory calculation to determine. The moment in the Fe muffin-tin sphere is about $1.8\mu_B$ for the two checkerboard orders, and about $2.0\mu_B$ for the two striped orders. The total moment for one Fe atom is estimated to be a little larger for the striped AF orders. For the striped AF orders, the Se position parameter remains almost the same

Table 1. The magnetic order, the relative total energy per formula unit (ΔE in meV, with the lowest stripe-FM set as reference), the magnetic moment in the Fe muffin-tin sphere (M in μ_B), and the internal Se position parameter u_{Se} of the two striped antiferromagnetic orders and the two checkerboard ones. The results of the nonmagnetic order are presented for comparison.

Magnetic order	ΔE (meV)	Moment M (μ_B)	u_{Se}
checkerboard-FM	72	1.82	0.2570
checkerboard-AF	72	1.81	0.2426
stripe-FM	0	1.98	0.2590
stripe-AF	5	2.00	0.2592
nonmagnetic	154	0.00	0.2471

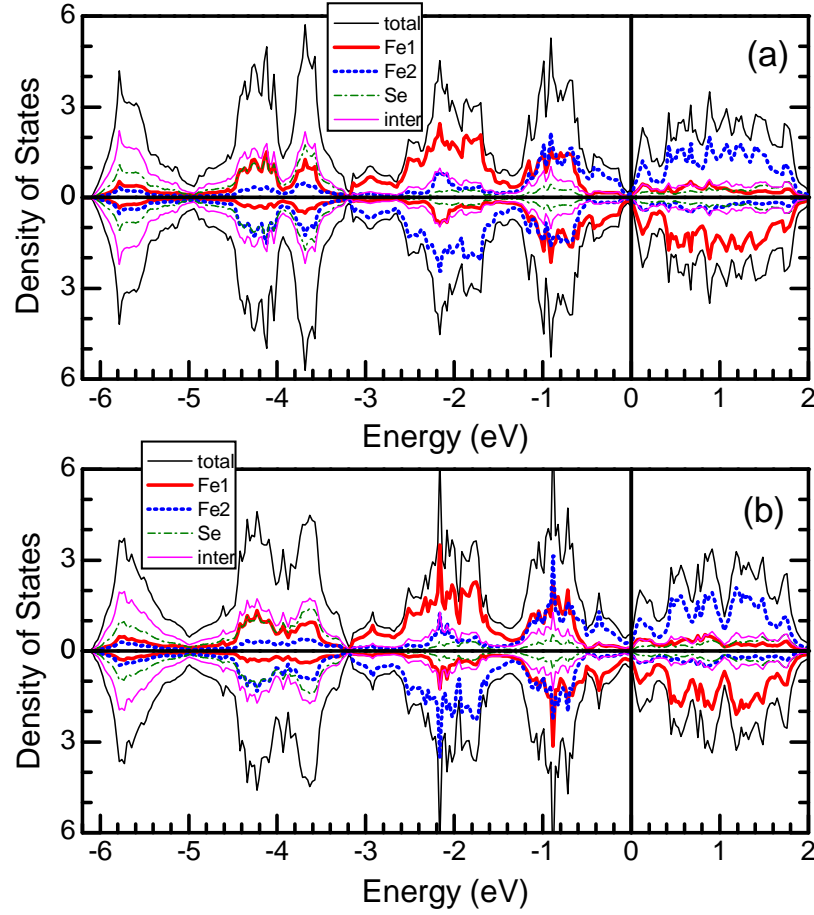


Figure 2. (color online). Spin-dependent density of states (DOS, in units of states/eV per formula unit) of the stripe-FM (a) and stripe-AF (b). The upper part of each panel is the majority-spin DOS and the lower part the minority-spin DOS. The Fe1 DOS is emphasized by thick red (or gray) solid lines, and the Fe2 DOS by thick blue (or gray) dotted lines. The black thin solid line indicates the spin-dependent total DOS, and the others are projected DOS in the muffin tin sphere of Se atom (dot-dash) and the interstitial region (pink or gray thin solid).

when the interlayer spin coupling is changed from FM to AF. Because it is impossible to distinguish between FM and AF spin alignment in the z direction by density-functional-theory calculation, we present calculated results for both FM and AF arrangement in the z direction in the following.

We present the spin-dependent density-of states (DOS) of the FeSe in the two striped AF orders in Fig. 2. There is no energy gap near the Fermi levels and therefore the FeSe for each AF order shows a metal feature. The Fe atom has different crystalline environment for different magnetic orders, and thus its states are reformed in different ways. It can be seen that the main peaks occupy the states in the energy window from -2.2 eV to -1.5 eV. Almost all the partial DOS of Fe atom comes from the 3d states, and the DOS of Se atom consists mainly of the p states.

We present the electronic energy bands of the FeSe in the two striped AF orders in

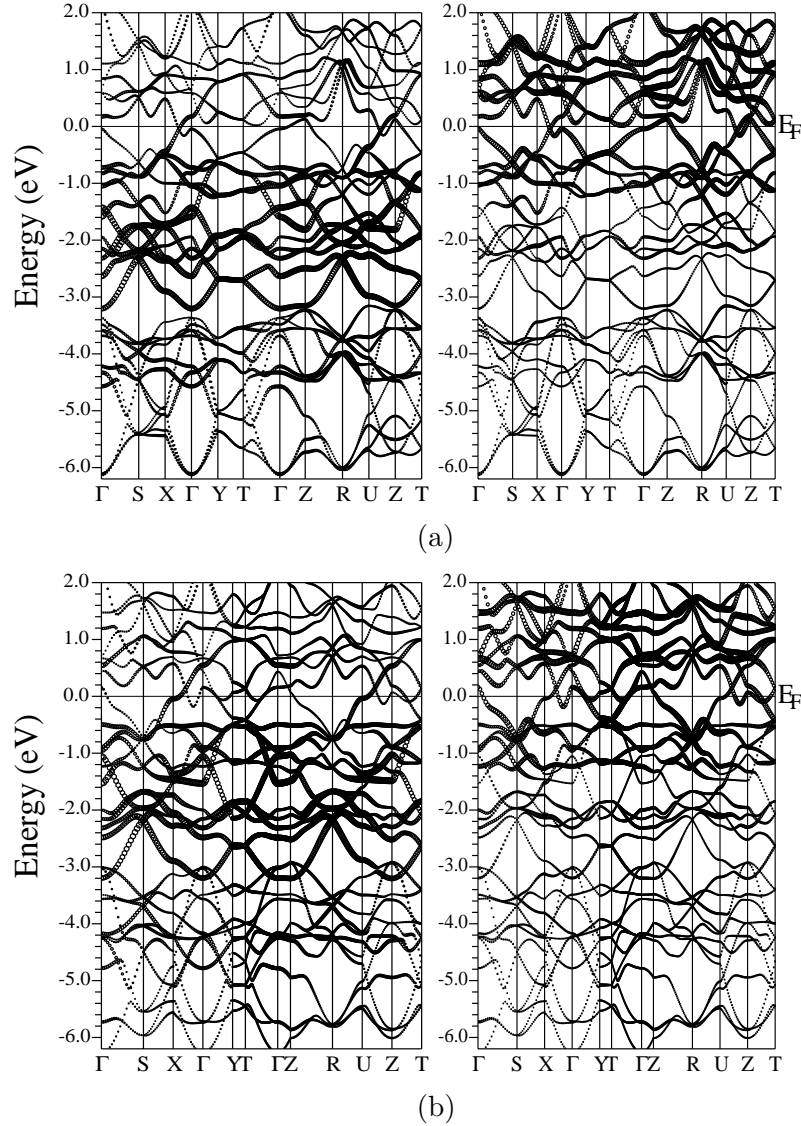


Figure 3. Spin-dependent energy bands of the stripe-FM (a), and stripe-AF (b). The left panel for each magnetic order shows the energy bands of Fe1 spin-up channel with the Fe1 atomic character emphasized by circles, and the right one those of Fe1 spin-down channel. The spin of Fe1 orients in antiparallel to that of Fe2. The emphasized energy bands consist of circles with different diameters, and the larger the diameter, the more the atomic character. There are so many circles (or dots) for a given band that they seem to be connected forming a line for the band.

Fig. 3. The plots look like lines, but consist of hollow circles. We choose the k points uniformly for convenient comparison. The circle diameter is proportional to the Fe1 spin-up or Fe1 spin-down atomic character of the band at that k point. The dispersion along the z direction is much stronger than those in other similar Fe-based materials. This can be attributed to the short distance between the successive Fe layers. It can be seen that the d states of Fe play a key role for all the magnetic structures. For

the stripe magnetic structures we can find the electrons and holes along the X- Γ -Y line, which is very important to achieving superconductivity in doped cases or under appropriate pressures.

4. Spin interactions and many-body effects on the magnetic moments

In order to further investigate the magnetic moment, we use the following AFM Heisenberg spin model to describe the spin properties of the Fe atoms in the striped AFM phase.

$$H = \sum_{ij} J_{ij} \vec{S}_i \cdot \vec{S}_j \quad (1)$$

where \vec{S}_i is quantum spin operator for site i , and J_{ij} is the exchange coupling constants between the two spins at sites i and j . For the striped AFM phase, the nearest coupling constant in the x direction is J_x , and that in the y direction J_y . For the tetrahedral phase, we should have $J_x = J_y$, but for the striped phase we have $J_x \neq J_y$ because the crystalline distortion in the xy plane. We limit non-zero exchange coupling constants up to the next nearest neighboring spins, J' . For convenience, we define $J = (J_x + J_y)/2$ and $\delta = J_x - J_y$. Our DFT calculation yields $J_x = 10\text{meV}$, $J_y = 8\text{meV}$, and $J' = 5\text{meV}$. These means $J = 9\text{meV}$ and $\delta = 2\text{meV}$. The J_x and J_y comes from the superexchange through the two nearest Se atoms and J' from that through the one nearest Se atom, and as a result, we should have $J \approx 2J'$, which supports our DFT results.

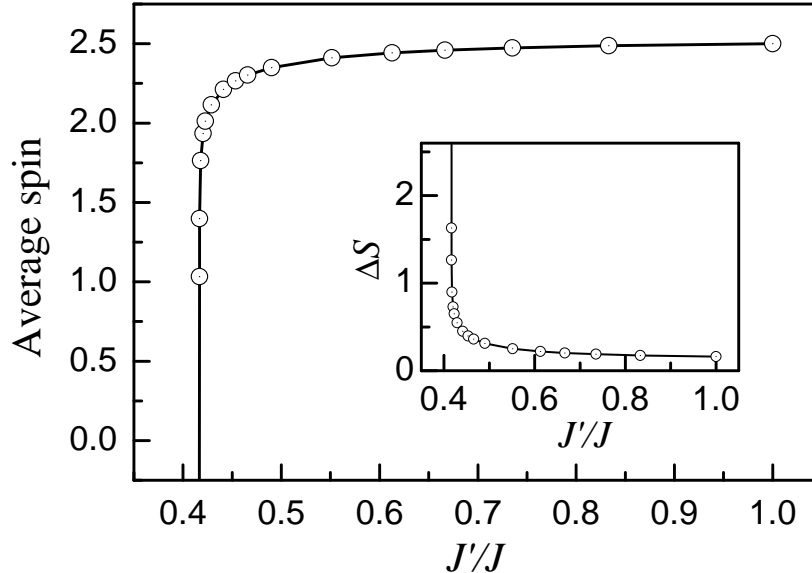


Figure 4. Zero-temperature average spin $\langle S^z \rangle$ vs. the coupling constant ratio J'/J for the two-dimensional spin model. The inset shows ΔS (defined in text) vs. J'/J . The \odot signs indicate calculated points.

We treat the spin Hamiltonian (1) with the above parameters with spin wave theory[30]. As usual, the average spin for zero temperature, $\langle S^z \rangle$, can be given by

$\langle S^z \rangle = S - \Delta S$, where S is the spin value of the Fe atom in the FeSe and ΔS the correction due to quantum many-body effects. Presented in Fig. 4 are our calculated results for $\langle S^z \rangle$ and ΔS as functions of the parameter J'/J . It is clear that $\langle S^z \rangle$ decreases with decreasing J'/J , getting to zero at $J' = J_y/2$. In fact, the striped AFM structure is not the magnetic ground state of the FeSe any more if J' is smaller than $J_y/2$. For real samples of the FeSe, one should have the parameter relations $J' \approx J/2$ and δ is small but finite, and therefore the experimental spin value is small compared to the DFT value S .

5. Conclusion

In summary, we have used the full-potential density-functional-theory method to study various magnetic orders and their effects on the electronic structures of the FeSe. We find that, for the spins of the single Fe layer, the striped antiferromagnetic orders with the broken symmetry are more favorable in total energy than the checkerboard antiferromagnetic orders with tetragonal symmetry, and the inter-layer magnetic interaction is very weak. Then, we investigate the corresponding electronic structures and magnetic property of the distorted phases with the striped antiferromagnetic orders. Our calculated result that the striped antiferromagnetic order is favorable for the spins of the Fe layer is consistent with main known experimental data. We also present our calculated spin coupling constants and conclude that the reduction of the Fe magnetic moment is caused by quantum many-body effects. These results are useful to understand the structural, magnetic, and electronic properties of FeSe, and may have some helpful implications to other FeAs-based materials.

Acknowledgements

This work is supported by Nature Science Foundation of China (Grant Nos. 10774180, 10874232, and 60621091), by Chinese Department of Science and Technology (Grant No. 2005CB623602), and by the Chinese Academy of Sciences (Grant No. KJCX2.YW.W09-5).

References

- [1] Y. Kamihara, T. Watanabe, M. Hirano, and H. Hosono, *J. Am. Chem. Soc.* **130**, 3296 (2008).
- [2] H. Takahashi, K. Igawa, K. Arii, Y. Kamihara, M. Hirano, and H. Hosono, *Nature* **453**, 376 (2008).
- [3] X. H. Chen, T. Wu, G. Wu, R. H. Liu, H. Chen, and D. F. Fang, *Nature* **453**, 761 (2008).
- [4] Z.-A. Ren, W. Lu, J. Yang, W. Yi, X.-L. Shen, Z.-C. Li, G.-C. Che, X.-L. Dong, L.-L. Sun, F. Zhou, and Z.-X. Zhao, *Chin. Phys. Lett.* **25**, 2215 (2008).
- [5] M. Rotter, M. Tegel, and D. Johrendt, *arXiv:0805.4630* (2008).
- [6] K. Sasmal, B. Lv, B. Lorenz, A. M. Guloy, F. Chen, Y.-Y. Xue, and C.-W. Chu, *arXiv:0806.1301* (2008).
- [7] P. L. Alireza, J. Gillett, Y. T. Chris Ko, S. E. Sebastian, and G. G. Lonzarich, *arXiv:0807.1896* (2008).

- [8] M. J. Pitcher, D. R. Parker, P. Adamson, S. J. C. Herkelrath, A. T. Boothroyd, and S. J. Clarke, arXiv:0807.2228 (2008).
- [9] C. de la Cruz, Q. Huang, J. W. Lynn, J. Li, W. Ratcliff II, J. L. Zarestky, H. A. Mook, G. F. Chen, J. L. Luo, N. L. Wang, and P. Dai, *Nature* **453**, 899 (2008).
- [10] S. Ishibashi, K. Terakura, and H. Hosono, *J. Phys. Soc. Jpn.* **77**, 053709, (2008).
- [11] Z. P. Yin, S. Lebegue, M. J. Han, B. P. Neal, S. Y. Savrasov, and W. E. Pickett, *Phys. Rev. Lett.* **101**, 047001 (2008).
- [12] T. Yildirim, *Phys. Rev. Lett.* **101**, 057010 (2008).
- [13] D. J. Singh and M. H. Du, *Phys. Rev. Lett.* **100**, 237003 (2008).
- [14] I. I. Mazin, D. J. Singh, M. D. Johannes, and M. H. Du, *Phys. Rev. Lett.* **101**, 057003 (2008).
- [15] A. S. Sefat, M. A. McGuire, B. C. Sales, R. Jin, J. Y. Howe, and D. Mandrus, *Phys. Rev. B* **77**, 174503 (2008).
- [16] Y. Mizuguchi, F. Tomioka, S. Tsuda, T. Yamaguchi, and Y. Takano, *Appl. Phys. Lett.* **93**, 152505 (2008).
- [17] L. Li, Z. R. Yang, M. Ge, L. Pi, J. T. Xu, B. S. Wang, Y. P. Sun, and Y. H. Zhang, arXiv:0809.0128 (2008).
- [18] S. B. Zhang, Y. P. Sun, X. D. Zhu, X. B. Wang, G. Li H. C. Lei, X. Luo, Z. R. Yang, W. H. Song, and J. M. Dai, arXiv:0908.1905 (2008).
- [19] K. W. Lee, V. Pardo, and W. E. Pickett, arXiv:0808.1733 (2008).
- [20] A. Subedi, L. Zhang, D. J. Singh, and M. H. Du, arXiv:0807.4312 (2008).
- [21] S. Matsuishi, Y. Inoue, T. Nomura, M. Hirano, and H. Hosono, arXiv:0810.2351v1 (2008).
- [22] X. Y. Zhu, F. Han, P. Cheng, G. Mu, B. Shen, and H. H. Wen, arXiv:0810.2531 (2008).
- [23] M. Tegel, S. Johansson, V. Weiss, I. Schellenberg, W. Hermes, R. Pottgen, and D. Johrendt, arXiv:0810.2120v1 (2008).
- [24] F. Han, X. Y. Zhu, G. Mu, P. Cheng, and H. H. Wen, arXiv:0810.2475v1 (2008).
- [25] L.-F. Zhu and B.-G. Liu, arXiv:0810.5049v1 (2008).
- [26] P. Hohenberg and W. Kohn, *Phys. Rev.* **136**, B864 (1964); W. Kohn and L. J. Sham, *Phys. Rev.* **140**, A1133 (1965).
- [27] P. Blaha, K. Schwarz, P. Sorantin, and S. B. Trickey, *Comput. Phys. Commun.* **59**, 399 (1990).
- [28] J. P. Perdew, K. Burke, and M. Ernzerhof, *Phys. Rev. Lett.* **77**, 3865 (1996).
- [29] D. D. Koelling and B. N. Harmon, *J. Phys. C: Solid St. Phys.* **10**, 3107 (1977).
- [30] B.-G. Liu, *Phys. Rev. B* **41**, 9563 (1990); B.-G. Liu, F.-C. Pu, G. Czycholl, *J. Magn. Magn. Mater.* **154**, 369 (1996).